Orthogonal frequency division multiplexing system with an indexed-pilot channel estimation

Ali Alqatawneh

Department of Computer and Communications Engineering, Faculty of Engineering, Tafila Technical University, Tafila, Jordan

Article Info

ABSTRACT

In this paper, we examine an orthogonal frequency division multiplexing (OFDM) system under imperfect channel conditions and pilot-aided-based channel estimation. However, unlike conventional pilot-aided-based channel estimation schemes, some inserted pilot symbols are set to zero where the indices of the zero-pilot symbols are employed to transmit extra data bits. In this paper, we employ a minimum mean squared error (MMSE) to detect transmitted pilot symbols; the detected pilot symbols are then used to estimate channel coefficients. Furthermore, the impacts of zero-pilot symbols on the mean-squared error of channel estimation and on system error performance are examined. Our findings show that the indices of zero-pilot symbols can be used to improve system throughput by carrying extra information bits without harming channel estimation accuracy or degrading system error performance. Simulation results show that, at a high signal-to-noise ratio, the bit error rate for data bits transmitted via zero-pilot symbols indices is lower than that of data bits transmitted over data subcarriers.

Corresponding Author:

Ali Alqatawneh
Department of Computer and Communications Engineering, Faculty of Engineering
Tafila Technical University
Tafila, Jordan
Email: ali.qatawneh@ttu.edu.jo

1. INTRODUCTION

Orthogonal frequency division multiplexing (OFDM) is a multi-carrier modulation technique widely implemented in broadband wireless communication systems such as long-term evolution (LTE) and all of the most recent Wi-Fi standards due to its high spectral efficiency and robustness when operating in frequency selective fading environments [1]. On the other hand, erroneous channel estimation is a crucial issue for wireless communication systems operating in frequency-selective fading channels, since channel-estimation errors might lead to considerable performance loss [2]. Moustakas *et al*. [3] show that, for larger spatially-correlated channels, the rate of performance degradation caused by channel estimation errors becomes more significant; this behavior becomes more apparent as the signal-to-noise ratio (SNR) rises. Several estimation techniques have been proposed to track channel variations to acquire precise channel-state information (CSI) [4]. Pilot-based channel estimation techniques are commonly used in wireless systems [5]. It is shown in [6] that the pilot patterns employed in OFDM systems for channel estimation determine the number of pilot symbols necessary to satisfy the targeted error performance. The minimum mean-squared error (MMSE) and the least-squared (LS) techniques are widely used along with pilot-based channel estimation schemes [7]-[15]. For example, Sun and Wu [7] investigate pilot-insertion channel estimation with the MMSE estimator and identify the optimal-pilot percentage that results in the maximum spectral efficiency. The pilot-symbol spacing can be optimized based on pilot density, Doppler spectrum, and power delay profile [8]. The mean-

squared error (MSE) of channel estimation can be reduced by either increasing the pilot percentage or rising the allocated energy to pilot symbols [9]. The asymptotic mean-square error of channel estimation, with pilot-insertion, is derived in [10] for high mobility wireless communication systems. According to [10], if the pilot sampling rate is equal to or greater than twice the maximum Doppler spread of the fading channel, then the MSE of the MMSE estimator at pilot-symbol and data-symbol locations are the same. A Pilot-insertion channel estimation scheme with an LS estimator was presented in [11] for different areas. Compared to the LS estimator, the MMSE estimator has a high level of complexity [12]. However, in terms of performance, the MMSE estimator out performs the LS [13]–[15]. An adaptive filter channel estimation scheme for multi-input-multi-output OFDM (MIMO-OFDM) systems is proposed in [16], where the authors show that the performance of MIMO-OFDM systems improves when coding and channel estimation are combined.

The idea behind index modulation is to improve the system spectral efficiency by sending extra information bits using: the indices of active subcarriers, the indices of transmitting or receiving antennas, or the index of matched impedance between the transmitter and receiver [17]–[19]. The OFDM with index modulation (OFDM-IM) technique is a novel multi-carrier modulation that conveys data bits using indices of active subcarriers and traditional symbol constellations [18], [19]. Furthermore, under various channel circumstances, the OFDM-IM system provides a considerable error-performance improvement compared to the classical OFDM systems [18]. Basar *et al.* [19] investigate an OFDM-IM system in high mobility conditions where their results show that the error performance of the OFDM-IM system surpasses that of the classical OFDM system under identical realistic channel conditions. Results obtained in [20], [21] indicate that an OFDM system with interleaved subcarrier index modulation (OFDM-ISIM) can enhance the system coding gain. Besides, the channel correlation of subcarriers in each subblock is independent when applying the subcarrier interleaving approach, resulting in the highest possible coding gain for OFDM-ISIM compared to OFDM-adjacent subcarrier index modulation (OFDM-ASIM). To improve the error performance of the OFDM-ISIM system, two different power allocation algorithms are suggested in [22]: the optimal and suboptimal power allocation algorithms. The first algorithm is designed by minimizing the pairwise error probability, whereas the second one is based on minimizing the Euclidean distance; however, the second algorithm has less computation complexity compared to the first one. An enhanced OFDM-IM system, where a single data bit determines the status of two successive subcarriers whether active or not, is proposed in [23] over a noisy channel; the proposed system improves the detection probability of active subcarriers at the receiver side. However, the spectral efficiency of the enhanced OFDM-IM system shows degradation compared to conventional OFDM-IM. To improve the OFDM system spectral efficiency, Li *et al.* [24] propose a channel estimation scheme where pilot locations are used to transmit additional data bits.

In this paper, we propose an OFDM system with a pilot-insertion-based channel estimation scheme and jointly MMSE pilot symbol detection and channel estimation. In the proposed system, pilot symbols are inserted among data symbols for channel estimation purposes, where some pilot symbols are set to zero. The index of zero-pilot symbols is used to convey extra data bits to enhance the throughput of the OFDM system. Furthermore, we employ the MMSE estimator to detect the transmitted pilot symbols and to estimate channel coefficients. We also, investigate the impact of the number of zero-pilot symbols on the estimation MSE and on the overall system error performance. The remainder of this article is presented as follows: Section 2 introduces the proposed system model. Section 3 presents results and discussion. Finally, section 4 concludes this article. The following notations are used all over the paper: $C(N, m)$ denotes the binomial coefficient, $\lfloor \ \rfloor$ represents the floor function, $\otimes$ represents the Kronecker product operator, and E is the mathematical expectation. Also, I_N represents the identity matrix of size N, $\mathbf{0}_{K \times 1}$ denotes a column vector of length K and zero elements, and $\boldsymbol{\beta}_{1 \times N}$ represents a row vector of length N and zero elements except for the last element, which equals to one. Finally, $()^H$ and $()^T$ denote the Hermitian and the transpose operations, respectively.

2. PROPOSED SYSTEM MODEL

In this paper, we consider an OFDM system with an indexed-pilot channel estimation (IPCE) scheme operating in a frequency-selective Raleigh fading channel. In the IPCE scheme, some pilot symbols are set to zero and the index of zero-pilot symbols is utilized to transmit extra data bits. In a classical pilot-channel estimation (CPCE) scheme, the data bits are mapped into M-array modulated symbols before adding a non-zero pilot symbol (or active pilot symbol) after every K-data symbol. The resulting symbol sequence contains N_s symbols where $N_s = KN + N$, with N being the number of pilot symbols in each sequence. However, in the proposed OFDM with IPCE scheme, a group of data bits is split into two parts: d-data bits and b-data bits. The data bits in the first part are mapped into M-array modulated symbols. In contrast, the data bits in the second part specify the indices of the zero-pilot symbols. The relationship between b, N, and m can be expressed as $b = \lfloor \log_2(C(N, m)) \rfloor$, with m being the number of zero-pilot (or inactive pilot) symbols. In other words, for b data bits, there will be 2^b different pilot-symbols realizations chosen from pilot

realization set **P** where the symbol corresponding to the inactive-pilot symbol is set to zero. For example, for $N=4$ and $m=2$, the number of transmitted bits via the indices of zero-pilot symbols is $b = \lfloor \log_2(C(4,2)) \rfloor = 2$ bits and the number of a pilot realizations will be $2^b=2^2=4$. An example of pilot-realization set is illustrated in Table 1.

Table 1. Pilot-realization set of OFDM with IPCE scheme for $N=4, m=2$

Data bits	Corresponding zero-pilot index	Corresponding pilot vector
[0 0]	{1,2}	[0, 0, p (3), p (4)]
[0 1]	{2,3}	[p (1), 0, 0, p (4)]
[1 0]	{3,4}	[p (1), p (2), 0, 0]
[1 1]	{1,4}	[0, p (2), p (3), 0]

For convenience, we only consider a binary phase-shift keying (BPSK) for data and active-pilot symbols. Also, we use OFDM-IPCE and OFDM-CPCE to refer to an OFDM system with IPCE scheme and to the OFDM system with CPCE scheme, respectively. After inserting the selected pilot symbols among data symbols, a symbol sequence, **s**, with length N_s is formed and can be expressed in vector format as [25]:

$$s = (s_d C_d + p C_p)^T \tag{1}$$

where the vector **s** is a column vector representing the data symbols after pilot-symbols insertion and serial-to-parallel conversion, $s_d = [s_d(1), s_d(2), \dots, s_d(NK)] \in \{-1,1\}$ is the data-symbol row vector before padding the pilot symbols, $p = [p(1), p(2), \dots, p(N) \in \{0, 1, -1\}]$ is a pilot-symbol row vector selected from 2^b-element pilot realization set; $C_d = I_N \otimes [I_K | 0_{K \times 1}]$ and $C_p = I_N \otimes \beta_{1 \times (K+1)}$ are the pilot-symbol padding matrices with sizes of $NK \times N_s$ and $N \times N_s$, respectively. For illustration, the block diagram of the OFDM-IPCE transmitter and the transmitted data slot, after pilot insertion, are shown in Figure 1. Figure 1(a) shows the OFDM-IPCE transmitter where the information bits are split into two groups. One group feeds binary bits to the BPSK mapper, and the second is sent to a pilot selector. Figure 1(b) shows a graphical representation for data symbols after padding the pilot symbols for a system with $K=3$, $N=4$, $m=2$, and $p = [0, p(2), p(3), 0]$ where $p(2)$ and $p(3) \in \{-1,1\}$.

(a)

(b)
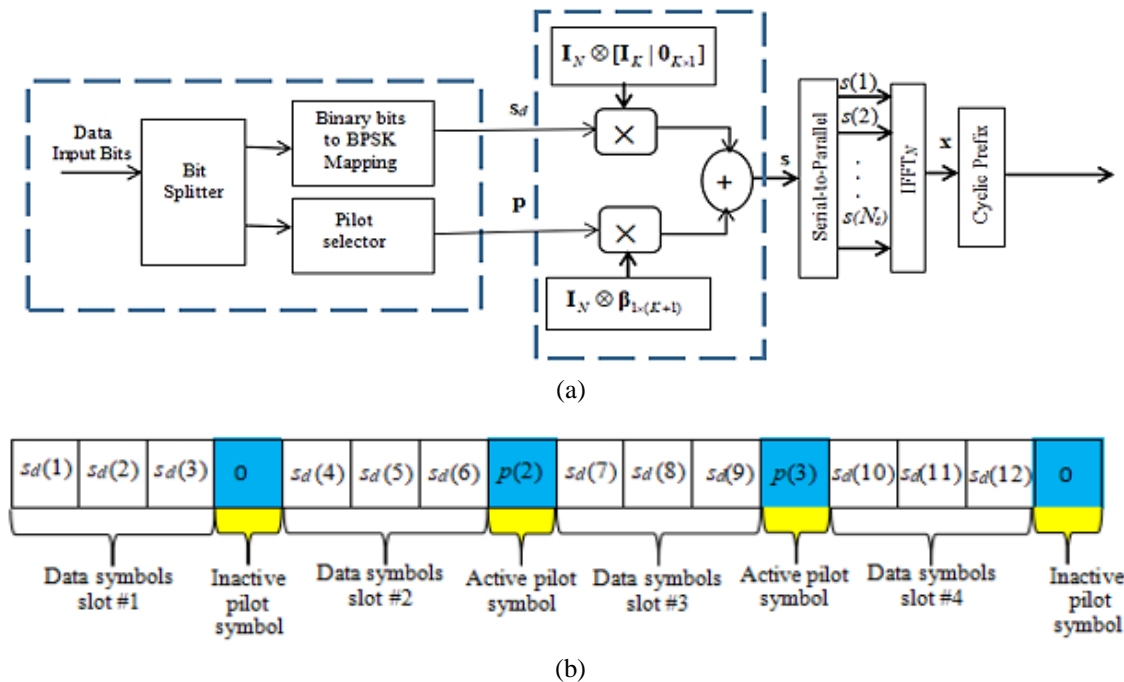
Figure 1. Illustration showing (a) OFDM-IPCE transmitter block diagram and (b) data symbols after pilot-symbols insertion

As in the classical OFDM system, the time-domain samples of the OFDM-IPCE system are acquired by taking the inverse fast fourier transform (IFFT) of the generated symbol sequence given in (1) using the inverse discrete fourier transform (IDFT) matrix D_N^H, i.e., $x = \text{IFFT}(s) = D_N^H s$, with $D_N^H D_N = N I_N$. At the output of the IFFT and after parallel to serial conversion, a cyclic prefix, with length L, is appended to the time-domain samples to eliminate inter symbol interference. After digital-to-analog conversion, the OFDM signal is transmitted over a frequency-selective Rayleigh fading channel. The input-output relationship of the observed signal at the receiver can be given in a discrete form and time-domain representation as [26]:

$$z = H_t \cdot x + n \tag{2}$$

where H_t is the time-domain channel matrix, and n is the time-domain noise vector. The frequency-domain representation of the received signal, given in (2), can be obtained by computing the fast fourier transform (FFT) of z using the discrete fourier transform (DFT) matrix, D_N, as shown [27]:

$$y = H_f s + w \tag{3}$$

where $y = D_N z$, $H_f = D_N H_t D_N^H$, and $w = D_N n$ are the observed signal samples at the receiver in the frequency domain, the frequency-domain channel matrix, and the frequency-domain noise vector at the receiver, respectively. The channel matrix, H_f, becomes a diagonal matrix if the channel undergoes quasi-static frequency selective fading as we considered in our system [27].

2.1. Pilot-symbol detection and channel estimation for the proposed system

In this subsection, we illustrate the way we employ the MMSE for joint pilot-symbol detection and channel coefficients estimation. Also, the estimation of channel coefficients associated with data symbols transmitted over data subcarriers is presented through this subsection. From the observed signal at the receiver, the signal at pilot-symbol locations can be extracted as (4):

$$y_p = C_p y \tag{4}$$

in terms of channel-coefficient vector at pilot-symbol positions, h_p, the (4) can be rewritten as (5):

$$y_p = S_p \cdot h_p + w_p \tag{5}$$

where S_p is a diagonal matrix with vector p on its main diagonal, i.e., $S_p = \text{diag}\{p\}$, and w_p is the frequency-domain noise vector at pilot-symbol positions. The auto-correlation matrix of channel coefficients at pilot-symbol positions can be expressed as $R_{pp} = E[h_p h_p^H]$. Based on [28], define the MMSE estimation matrix, G_p, as $G_p = \widetilde{R}_{pp}(\bar{R}_{pp} + N_o I_N)^{-1}$. The matrix $\widetilde{R}_{pp}$ can be derived from R_{pp} by replacing all its columns having the same inactive-pilot symbols indices with zeros. Likewise, $\bar{R}_{pp} = S_p R_{pp} S_p^H$ can be obtained from R_{pp} by replacing its columns and rows having the same inactive-pilot symbols indices with zeros. Using the channel-estimation matrix, G_p, channel coefficients at pilot positions can be estimated as (6):

$$\widehat{h}_p = G_p y_p = \widetilde{R}_{pp}(\bar{R}_{pp} + N_o I_N)^{-1} y_p \tag{6}$$

if we express the estimated channel vector, $\widehat{h}_p$, as: $\widehat{h}_p = h_p + e_p$, where $e_p = [\, e_p(1),\, e_p(2),\ldots,\, e_p(N)]$ is the estimation error vector, the expectation value of the exact channel vector at pilot positions conditioned on its estimated version is then $E[h_p/\widehat{h}_p] = E[(h_p - e_p)/\widehat{h}_p] = \widehat{h}_p$ [29]. Furthermore, the observed signal at pilot positions conditioned on both $\widehat{h}_p$ and p, i.e. $(y_p/\widehat{h}_p, p)$, is Gaussian random variable with conditional mean and conditional variance given respectively as [30]:

$$u = S_p \widehat{h}_p \tag{7a}$$

$$R_e = E_p + N_o I_N \tag{7b}$$

where $E_p = E[e_p e_p^H]$ with the k-th element of the main diagonal being estimated as $E\left[|e_p(k)|^2\right]$.

Based on the above information, the probability density function (PDF) of the observed signal at pilot positions conditioned on both $\widehat{h}_p$ and p is given as (8) [30]:

$$p(y_p/\widehat{h}_p, p) = \frac{1}{\det(\pi(E_p + \frac{1}{\gamma}I_N))} exp\left[-\left(y_p - \text{diag}\{p\}\widehat{h}_p\right)^H (E_p + \frac{1}{\gamma}I_N)^{-1}\left(y_p - \text{diag}\{p\}\widehat{h}_p\right)\right] \quad (8)$$

where $1/\gamma = N_o$, and det is the matrix determinant. The error probability of pilot-symbols detection can be minimized by maximizing the likelihood function given in (8), and this can be done by choosing the pilot symbols such that [30];

$$\widehat{p} = \underset{p \in P}{\text{argmin}}\left(y_p - \text{diag}\{p\}\widehat{h}_p\right)^H (E_p + \frac{1}{\gamma}I_N)^{-1}\left(y_p - \text{diag}\{p\}\widehat{h}_p\right) \quad (9)$$

The MSE for vector $\widehat{h}_p$ estimate is given as [6]:

$$\Delta_p = \frac{1}{N}\text{tr}\{\mathbf{E}_p\} \quad (10)$$

where tr { } is the matrix trace. Alternatively, expression in (10) can be written as (11):

$$\Delta_p = \frac{1}{N}\Sigma \mathbf{V}\mathbf{\Lambda}\mathbf{V}^{-1} = \frac{1}{N}\Sigma\mathbf{\Lambda}\mathbf{V}\mathbf{V}^{-1} = \frac{1}{N}\Sigma\mathbf{\Lambda}\mathbf{I}_N = \frac{1}{N}\sum_{k=1}^{N}\lambda_k \quad (11)$$

the MSE, Δ_p, in (11) is derived by performing eigenvalue decomposition for the error matrix, $\mathbf{E}_p$, as $\mathbf{E}_p = \mathbf{V}\mathbf{\Lambda}\mathbf{V}^{-1}$ where $\mathbf{V}$ is the eigenvector, and $\mathbf{\Lambda} = \text{diag}\{\lambda_1, \lambda_2, \dots, \lambda_N\}$ with λ_k being the k-th eigenvalue of $\mathbf{E}_p$ [31]. For large values of N, we can approximate $\mathbf{E}_p$ as $\mathbf{E}_p = \Delta_p\mathbf{I}_N$ and the estimated pilot symbols in (9) can be simplified to:

$$\widehat{p} = \frac{1}{\Delta_p + N_o}\underset{p \in P}{\text{argmin}}\left\|\left(y_p - \text{diag}\{p\}\widehat{h}_p\right)\right\|^2 \quad (12)$$

where for a column vector $\mathbf{b}$, $\|\mathbf{b}\|^2 = \mathbf{b}^H\mathbf{b}$.

After we estimate the pilot symbols and identify the indices of the inactive pilot symbols, we can estimate the channel coefficients for data symbols and use the calculated channel coefficients to conduct detection for data symbols sent over data subcarriers. The received signal at data-subcarrier locations can be retrieved from the observed signal, y, as (13):

$$y_d = C_d y = S_d \cdot h_d + w_d \quad (13)$$

where S_d, is a diagonal matrix with vector s_d on its main diagonal, w_d is the frequency-domain noise vector at data-subcarrier positions, and h_d is the channel coefficients at data-subcarrier positions. If we refer to the cross-correlation matrix of h_d and h_p as $R_{dp} = E[h_d h_p^H]$, then we can define the channel estimation matrix, G_d, as $G_d = \widetilde{R}_{dp}(\widetilde{R}_{pp} + N_o I_N)^{-1}$ where $\widetilde{R}_{dp} = R_{dp}\widehat{S}_p$, and $\widetilde{R}_{pp} = \widehat{S}_p R_{pp}\widehat{S}_p^H$ with $\widehat{S}_p = \text{diag}\{\widehat{p}\}$. The estimate of channel coefficients at data-subcarrier positions can be obtained as $\widehat{h}_d = G_d y_d$. The channel-estimation error matrix for channel estimation at data-carrier locations, E_d, is defined as (14):

$$E_d = E\left[(\widehat{h}_d - h_d)(\widehat{h}_d - h_d)^H\right] = R_{dd} - \widehat{R}_{dd} = R_{dd} - \widetilde{R}_{dp}(\widetilde{R}_{pp} + N_o I_N)^{-1}\widetilde{R}_{dp}^H \quad (14)$$

where $R_{dd} = E[h_d h_d^H]$. The k-th element of the main diagonal of matrix E_d can be calculated as $E\left[|\widehat{h}_d(k) - h_d(k)|^2\right] = E[|e_d(k)|^2]$. Given E_d, the MSE for channel estimation at data-carrier positions can then be calculated as (15):

$$\Delta_d = \frac{1}{KN}\sum_{k=1}^{KN}\phi_k \quad (15)$$

where ϕ_k is the k-th eigenvalue of the error matrix $\boldsymbol{E}_d$. For large N, the estimation-channel error matrix, $\boldsymbol{E}_d$, can be approximated as $\boldsymbol{E}_d = \Delta_d \boldsymbol{I}_{KN}$. Thus, the optimum detection rule for the k-th data symbol transmitted over data subcarrier can be obtained as [30]:

$$\hat{s}_d(k) = \frac{1}{\Delta_d + N_o} \underset{s_k \in \boldsymbol{S}}{\text{argmin}} \left(y_d(k) - \hat{h}_d(k)s_k \right)^H \left(y_d(k) - \hat{h}_d(k)s_k \right) \tag{16}$$

and this is equivalent to minimize the Euclidean distance between the observed signal sent over the k-th data subcarrier, $y_d(k)$, and the predicted one as (17):

$$\hat{s}_d(k) = \frac{1}{\Delta_d + N_o} \underset{s_k \in \boldsymbol{S}}{\text{argmin}} \left| \left(y_d(k) - \hat{h}_d(k)s_k \right) \right|^2 \tag{17}$$

Next, the error and throughput analysis will be presented.

2.2. Performance analysis of the proposed system

In this subsection we present the bit error rate of the proposed OFDM-IPCE system. Based on (12) in [28] the conditional bit error rate for the OFDM-IPCE system can be represented as (18):

$$P_k / \hat{h}_d(k) = \frac{1}{\pi} \int_0^{\frac{\pi}{2}} \exp\left(-\hat{h}_d(k) \left(\Delta_d + \frac{1}{\gamma} \right)^{-1} \hat{h}_d^H(k) \frac{1}{\sin(\emptyset)} \right) d\emptyset$$
$$= \frac{1}{\pi} \int_0^{\frac{\pi}{2}} \exp\left(-\alpha \left| \hat{h}_d(k) \right|^2 \frac{1}{\sin(\emptyset)} \right)^{-1} d\emptyset \tag{18}$$

where $\alpha = \Delta_d + 1/\gamma$. The term $\left| \hat{h}_d(k) \right|^2$ is a random variable with Chi-distribution and 2-degree of freedom. Thus, the unconditional bit error rate for data bits transmitted over the k-th data subcarrier in the OFDM-IPCE system can be obtained using the moment generating function shown in (19) in [30]. The result can then be described as (19):

$$P_k = \frac{1}{\pi} \int_0^{\frac{\pi}{2}} \left(1 + \frac{\alpha \sigma_d}{sin^2(\phi)} \right)^{-1} d\phi \tag{19}$$

where $\sigma_d = E \left| \hat{h}_d(k) \right|^2$. Using (19) the total bit-error rate for bits transmitted over data subcarriers can be given as (20).

$$P_T = \sum_{k=1}^{KN} P_k \tag{20}$$

2.1. Throughput analysis of the proposed system

Define a pilot-symbol percentage for the OFDM-IPCE system with BPSK bit-to-symbol mapping as the number of pilot symbols divided by the total number of transmitted data symbols which can be expressed as (21):

$$\rho_{IPCE}^p = \frac{N}{KN + \left\lfloor \log_2 \binom{N}{m} \right\rfloor} = \frac{1}{K + \frac{1}{N} \left\lfloor \log_2 \binom{N}{m} \right\rfloor} \tag{21}$$

similarly, define the pilot-symbol percentage for OFDM-CPCE system as (22).

$$\rho_{CPCE}^p = \frac{N}{KN} = \frac{1}{K} \tag{22}$$

Thus, from (21) and (22),

$$\rho_p = \frac{\rho_{IPCE}^p}{\rho_{CPCE}^p} = \frac{1}{1 + \frac{1}{NK} \left\lfloor \log_2 \binom{N}{m} \right\rfloor} \tag{23}$$

because the ratio in (23) is always less than one, we can conclude that the pilot symbol percentage decreases when using the IPCE scheme in OFDM. The percentage reduction depends on K, N, and the number of inactive pilot symbols, m. Now, define the information bit percentage for the proposed OFDM-IPCE as the number of the transmitted information bits divided by the total number of available active subcarriers:

$$\rho_{IPCE}^{i} = \frac{KN + \left\lfloor \log_2 \binom{N}{m} \right\rfloor}{KN + (N-m)} \tag{24}$$

and for the OFDM with a classical-pilot channel estimation, the information bit percentage becomes as (25):

$$\rho_{CPCE}^{i} = \frac{KN}{KN + N} = \frac{K}{K+1} \tag{25}$$

therefore,

$$\rho_i = \frac{\rho_{IPCE}^{i}}{\rho_{CPCE}^{i}} = \frac{KN + \left\lfloor \log_2 \binom{N}{m} \right\rfloor}{KN - mK} \tag{26}$$

according to (24)-(26), ρ_{IPCE}^{i} is always bigger than ρ_{CPCE}^{i}, and ρ_i is always greater than unity, implying that the OFDM-IPCE system always outperforms the OFDM-CPCE scheme in terms of system throughput.

3. RESULTS AND DISCUSSION

In this section, we present computer simulation results for the OFDM-IPCE system under various operating conditions. In all simulations, the BPSK constellation was adopted for both data and active pilot symbols. Figure 2 compares the mean-squared error, Δ_p, of channel estimation at pilot-symbol locations of the proposed OFDM-IPCE system with that of the OFDM-CPCE system under various numbers of pilot symbols; the value of Δ_p at $m=0$ belongs to OFDM-CPCE system. All plots obtained at $K=1$ and $\gamma=15$ dB. Figure 2 reveals that, for the same number of pilot symbols, the mean-squared error difference between the proposed OFDM-IPCE and OFDM-CPCE systems grows as the number of inactive-pilot symbols increases. However, in the OFDM-IPCE system and at the same number of inactive pilot symbols, increasing the number of pilot symbols, N, decreases the difference. For example, when $m=4$ and $N=48$, we can observe the maximum mean-squared error difference between the two systems, whereas, at $m=4$ and $N=8$, we can observe the minimum difference.
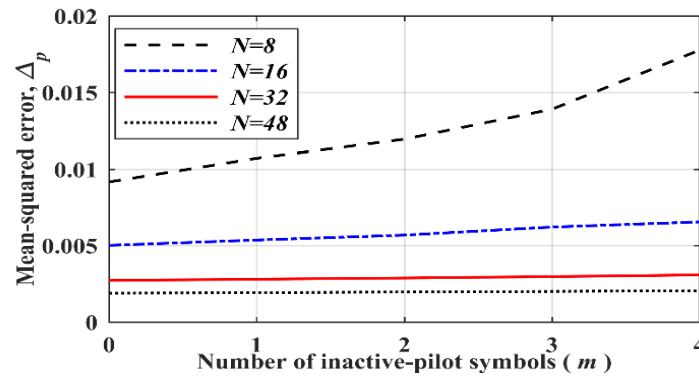
Figure 2. The MSE of channel estimation at pilot symbols as a function of inactive pilot symbols, m, for both OFDM-IPCE and OFDM-CPCE systems

In Figure 3, we plot the mean-squared error for channel estimation at pilot positions for OFDM-IPCE under different numbers of inactive pilots. All plots were generated for systems with $K=1$, $N=48$, and $\gamma=5$ dB. As previously stated, increasing the number of inactive pilots raises the number of transmitted information bits; yet, increasing the number of inactive pilots increases the MSE of channel estimation at pilot locations. This increase is proportional to the number of inactive-pilot symbols, m; as can be seen, the mean-squared error grows as m increases. For example, the maximum values of the Δ_p for OFDM with IPCE for $m=1$, $m=2$, $m=3$, and $m=4$ are 0.01454, 0.01486, 0.01511, and 0.01559, respectively. These results are near to the mean-squared error for a comparable OFDM-CPCE system, which equals $\Delta_p = 0.0142$.

The simulated bit error rate BER of data bits transmitted over the indices of inactive-pilot symbols, m, for the OFDM-IPCE system is plotted in Figure 4 for various numbers of inactive-pilot symbols. As

indicated in the Figure 4, at fixed number of pilot symbols, the BER for bits sent through pilot-symbol indices increases with any increase in the number of inactive-pilot symbols. Increasing the number of inactive-pilot symbols raises the number of available choices in pilot realization lookup-table, leading to an increase in pilot-symbol estimation errors. However, these errors can be reduced by increasing, γ, which means more power can be allocated to non-zero pilot symbols. Also, it should be noted that, increasing m increases the number of data bits transmitted through the indices of zero-pilot symbols.
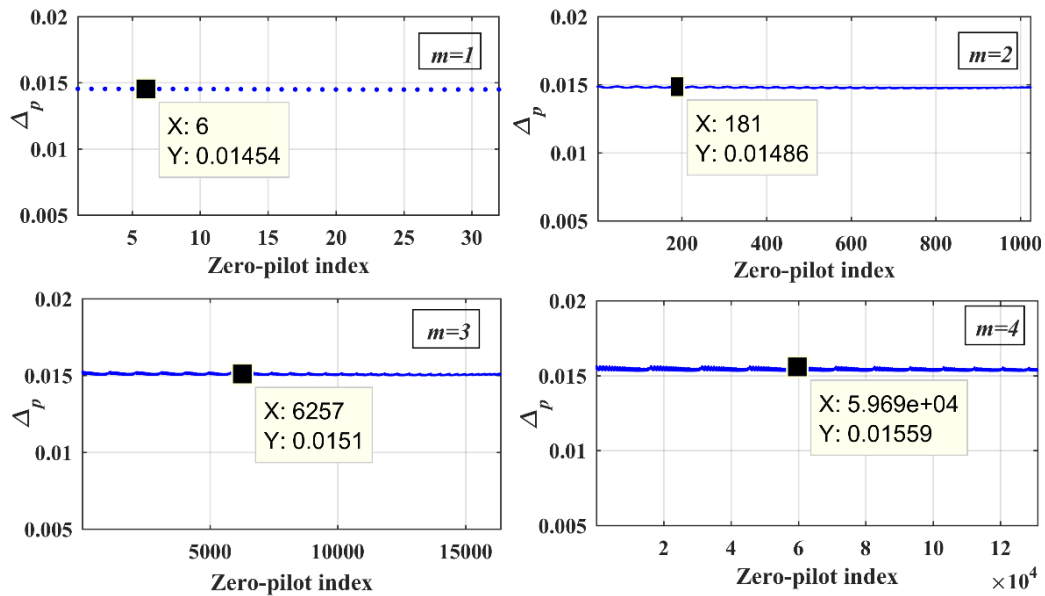
Figure 3. The mean-squared error of channel estimation at pilot positions of OFDM-IPCE system under different numbers of inactive-pilot symbols
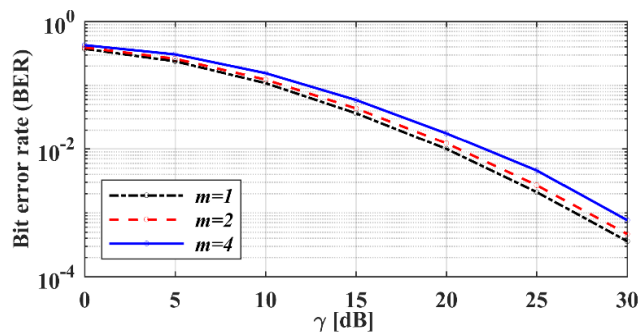
Figure 4. The BER of bits transmitted through inactive-pilot symbols indices as a function of signal-to-noise ratio, γ when $K=3$, and $N=16$

Figure 5 compares the total bit-error rate, P_T, for bits transmitted over data subcarriers in OFDM-CPCE and OFDM-IPCE systems with varying numbers of inactive pilot symbols, m, and under various system configurations. Furthermore, the bit error rate of the OFDM-CPCE and OFDM-IPCE systems are compared to identical systems with perfect channel state information (PCSI) at the receiver. We used $N=16$ for systems with channel estimation, for systems with PCSI we used $N_s=64$. As seen in the Figure 6, P_T for the OFDM-CPCE and OFDM-IPCE systems are comparable and very close to an equivalent OFDM system operating under PCSI. However, the transmitted data bits in the OFDM-IPCE system are greater than those in the OFDM-CPCE system when the same number of data subcarriers and active pilot subcarriers are used. For example, at $\gamma=35$ dB, the error performance at different values of inactive pilot symbols is almost identical and very close to the error performance of the OFDM-IPCE system at the same γ value.

In Figure 6, the error performance of OFDM-IPCE system is compared with that of OFDM-CPCE under various conditions. The BER for data bits transmitted over data subcarriers and the BER for data bits transmitted via the indices of inactive-pilot symbols are shown in Figure 6(a) for the OFDM-IPCE system. Also, the error performance for the OFMD-CPCE system is shown in Figure 6(b). It is clear from Figure 6(a) that the BER for data bits transmitted over data subcarriers is better than BER for data bits transmitted via pilot symbols indices. However, at a high SNR, the BER for bits transmitted over the indices of inactive pilots becomes better than the BER of bits transmitted over data subcarriers. In both OFDM-IPCE and OFDM-CPCE systems, the error performance for information bits sent over data subcarriers improves as the number of pilot symbols grows, as predicted, since increasing N reduces channel estimation errors, which leads to better BER.
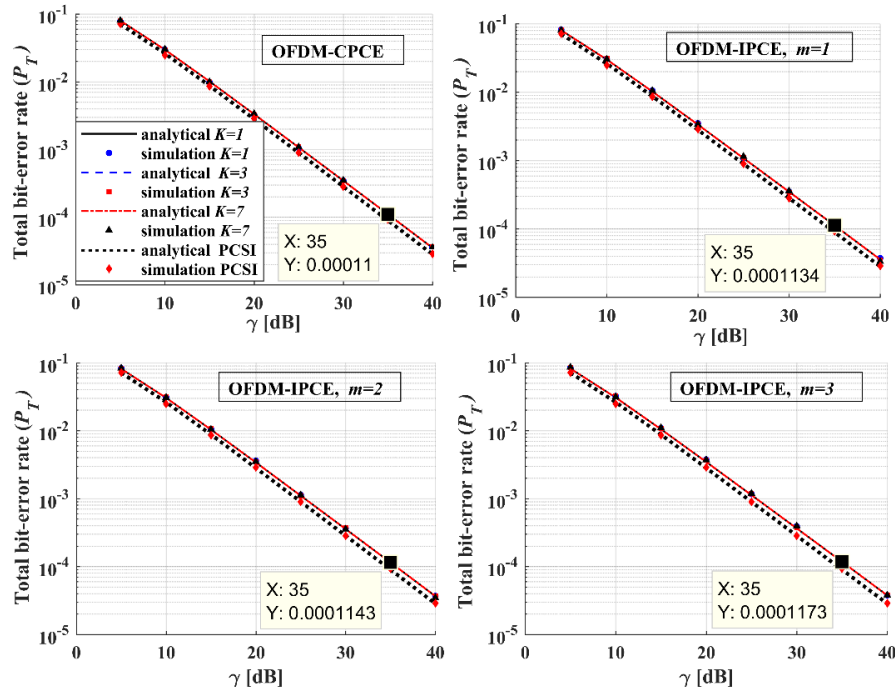
Figure 5. Total bit-error rate for bits transmitted over data subcarriers as a function of γ, and under different values of m
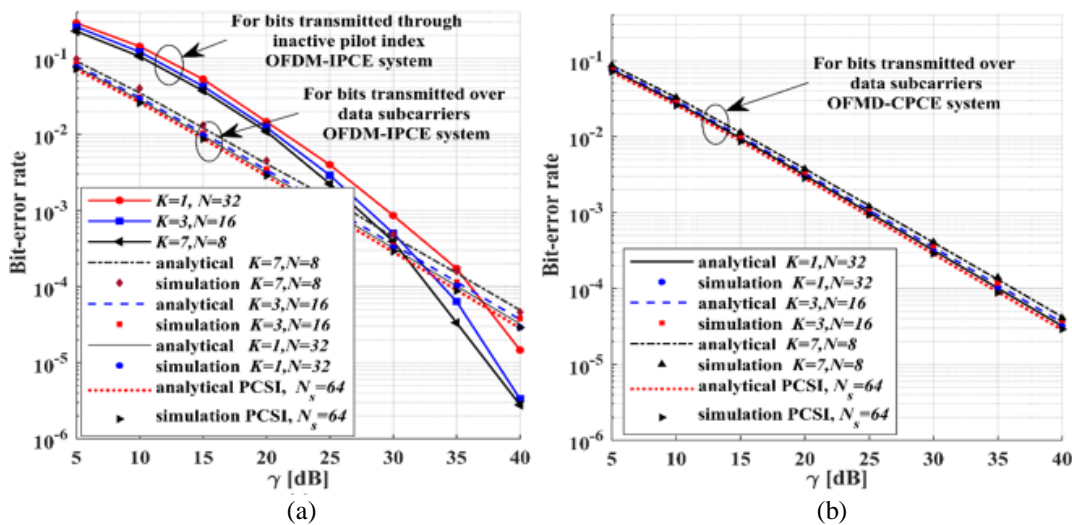
Figure 6. The error performance of OFDM-IPCE and OFDM-CPCE as afunction of γ under different system configurations for (a) OFDM-IPCE system when $m=2$ and OFDM-CPCE system where $m=0$

Comparing Figure 6(a) with Figure 6(b), we observe that the error performance for bits sent over the data subcarriers in OFDM-IPCE is comparable to that of OFDM-CPCE. However, under the same data slot length, K, number of pilot subcarriers, N, and SNR, γ, the system throughput for the OFDM-IPCE system is higher than that of the OFDM-CPCE system. Compared to the OFDM system with PCSI, the error performance of data bits transmitted over data subcarriers for both OFDM-IPCE and OFDM-CPCE systems show a significant improvement with the number of pilot symbols increasing. Finally, at a fixed number of zero-pilot symbols, the error performance for bits transmitted over the indices of these symbols shows improvement as the number of pilot symbols decreases.

Figure 7 shows the ratio of the transmitted information bits to the number of active subcarriers as a function of the number of inactive-pilot symbols under different numbers of pilot symbols and data slot lengths. Also, we compare the obtained percentage with that of the OFDM-CPCE system where $m=0$. From Figure 7, we can observe that the information bit percentage for the OFDM-PICE system is greater than that of the OFDM-CPCE system. For example, at $K=1$, $N=32$, and $m=8$, the information bit percentage is $\rho_{CPCE}^{i}=0.5$ for the OFDM-CPCE system and $\rho_{IPCE}^{i}=0.98210$ for the OFDM-IPCE system. In other words, at $K=1$, $N=32$, and $m=8$, we can send 55 information bits in OFDM-IPCE; however, the number of transmitted data bits drops to 32 in OFDM-CPCE system.
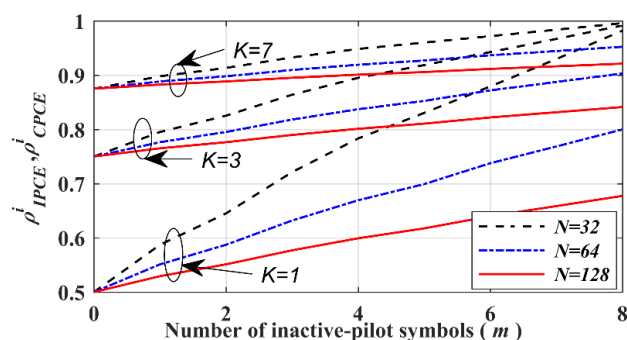
Figure 7. The ratio of the transmitted bits to the number of active subcarriers as a function of m for OFDM-IPCE and OFDM-CPCE

4. CONCLUSION

In this paper, we have studied an OFDM system with indexed pilot-aided channel estimation and MMSE-based pilot-symbol detection. Also, we have investigated the effect of the number of zero pilots on the mean-squared error of channel estimation and on bit error performance. Results have shown that the value of the mean-squared error depends on both the number of inactive-pilot symbols and the number of pilot symbols. For example, at a given number of inactive pilot symbols, increasing the number of pilot symbols reduces the mean-squared error of the system channel estimate. Furthermore, we have found that the BER for bits transmitted through the zero-pilot index outperforms the BER for information bits transmitted over data subcarriers at higher signal-to-noise ratios. Also, research has shown that the pilot symbols added for channel estimation can be used to send information bits without hurting the performance of channel estimation or the system error performance.

REFERENCES

[1]   A. Rafay, S. M. Idrus, K. M. Yusof, and S. H. Mohammad, "A survey on advanced transmission technologies for high bandwidth and good signal quality for high-speed railways," *Indonesian Journal Electrical Engineering and Computer Science*, vol. 23, no. 1, pp. 293–301, 2021, doi: 10.11591/ijeecs.v23.i1.pp293-301.

[2]   R. Mulyawan, R. Averly, I. Syafalni, N. Sutisna, and T. Adiono, "Dynamic pilot allocation for channel estimation in high-mobility OFDM receiver," *In 2021 International Conference on Electronics, Information, and Communication (ICEIC)*, 2021, pp. 1-4, doi: 10.1109/ICEIC51217.2021.9369750.

[3]   A. L. Moustakas, G. C. Alexandropoulos, A. Polydoros, I. Kaddas, and I. Dagres, "Impact of imperfect channel estimation in HF OFDM-MIMO communications," in *IEEE International Symposium on Personal, Indoor and Mobile Radio Communications, PIMRC*, vol. 2019-Septe, 2019, doi: 10.1109/PIMRC.2019.8904116.

[4]   Y. Liu, Z. Tan, H. Hu, L. J. Cimini, and G. Y. Li, "Channel estimation for OFDM," *IEEE Commun. Surv. Tutorials*, vol. 16, no. 4, pp. 1891–1908, 2014, doi: 10.1109/COMST.2014.2320074.

[5]   J. Sterba and D. Kocur, "Pilot symbol aided channel estimation for OFDM system in frequency selective rayleigh fading channel," in *Proceedings of 19th International Conference Radioelektronika 2009, RADIOELEKTRONIKA '09*, 2009, pp. 77–80, doi: 10.1109/RADIOELEK.2009.5158729.

[6]   F. Tufvesson and T. Maseng, "Pilot assisted channel estimation for OFDM in mobile cellular systems," in *IEEE Vehicular Technology Conference*, vol. 3, 1997, pp. 1639–1643, doi: 10.1109/vetec.1997.605836.

[7]   N. Sun and J. Wu, "Maximizing spectral efficiency with imperfect channel information in high mobility systems," in *GLOBECOM - IEEE Global Telecommunications Conference*, 2013, pp. 3359–3364, doi: 10.1109/GLOCOM.2013.6831591.

[8]   J. W. Choi and Y. H. Lee, "Optimum pilot pattern for channel estimation in OFDM systems," *IEEE Trans. Wirel. Commun.*, vol. 4, no. 5, pp. 2083–2088, 2005, doi: 10.1109/TWC.2005.853891.

[9]   N. Sun, J. Wu, and P. Fan, "Optimum designs of high mobility wireless systems with channel estimation errors," *IET Commun.*, vol. 9, no. 13, pp. 1677–1682, 2015, doi: 10.1049/iet-com.2014.0952.

[10] N. Sun and J. Wu, "Maximizing spectral efficiency for high mobility systems with imperfect channel state information," *IEEE Trans. Wirel. Commun.*, vol. 13, no. 3, pp. 1462–1470, Mar. 2014, doi: 10.1109/TWC.2014.012314.130772.

[11] H. A. J. Al-Asady, H. F. Fakhruldeen, and M. Q. Alsudani, "Channel estimation of OFDM in C-band communication systems under different distribution conditions," *Indonesian Journal Electrical Engineering and Computer Science*, vol. 23, no. 3, pp. 1778–1782, 2021, doi: 10.11591/ijeecs.v23.i3.pp1778-1782.

[12] A. Bahadur Singh and V. Kumar Gupta, "Performance evaluation of MMSE and LS channel estimation in OFDM system," *Int. J. Eng. Trends Technol.*, vol. 15, no. 1, pp. 39–43, 2014, doi: 10.14445/22315381/ijett-v15p209.

[13] M. B. Sutar and V. S. Patil, "LS and MMSE estimation with different fading channels for OFDM system," in *Proceedings of the International Conference on Electronics, Communication and Aerospace Technology, ICECA 2017*, vol. 2017-Janua, 2017, pp. 740–745, doi: 10.1109/ICECA.2017.8203641.

[14] J. A. Sam and A. K. Nair, "Analysis and implementation of channel estimation in OFDM system using pilot symbols," in *2016 International Conference on Control Instrumentation Communication and Computational Technologies, ICCICCT 2016*, 2017, pp. 725–728, doi: 10.1109/ICCICCT.2016.7988047.

[15] M. K. Abboud and B. M. Sabbar, "Performance evaluation of high mobility OFDM channel estimation techniques," *Int. J. Electr. Comput. Eng.*, vol. 10, no. 3, pp. 2562–2568, 2020, doi: 10.11591/ijece.v10i3.pp2562-2568.

[16] S. Pyla, K. P. Raju, and N. B. Subrahmanyam, "Performance analysis of adaptive filter channel estimated MIMO OFDM communication system," *Int. J. Electr. Comput. Eng.*, vol. 8, no. 5, pp. 3829–3838, 2018, doi: 10.11591/ijece.v8i5.pp3829-3838.

[17] H. Y. Lee and S. Y. Shin, "A novel index modulation scheme with impedance matching," *Indonesian Journal Electrical Engineering and Computer Science*, vol. 14, no. 3, pp. 1203–1209, 2019, doi: 10.11591/ijeecs.v14.i3.pp1203-1209.

[18] E. Basar, U. Aygolu, E. Panayirci, and H. V. Poor, "Orthogonal frequency division multiplexing with index modulation," *IEEE Trans. Signal Process.*, vol. 61, no. 22, pp. 5536–5549, Nov. 2013, doi: 10.1109/TSP.2013.2279771.

[19] E. Basar, U. Aygolu, and E. Panaylrcl, "Orthogonal frequency division multiplexing with index modulation in the presence of high mobility," in *2013 1st International Black Sea Conference on Communications and Networking, BlackSeaCom 2013*, vol. 61, no. 22, 2013, pp. 147–151, doi: 10.1109/BlackSeaCom.2013.6623399.

[20] Y. Xiao, S. Wang, L. Dan, X. Lei, P. Yang, and W. Xiang, "OFDM with interleaved subcarrier-index modulation," *IEEE Commun. Lett.*, vol. 18, no. 8, pp. 1447–1450, Aug. 2014, doi: 10.1109/LCOMM.2014.2332340.

[21] M. Wen, X. Cheng, M. Ma, B. Jiao, and H. V. Poor, "On the achievable rate of OFDM with index modulation," *IEEE Trans. Signal Process.*, vol. 64, no. 8, pp. 1919–1932, 2016, doi: 10.1109/TSP.2015.2500880.

[22] Q. Ma *et al.*, "Power allocation for OFDM with index modulation," in *IEEE Vehicular Technology Conference*, vol. 2017-June, 2017, doi: 10.1109/VTCSpring.2017.8108623.

[23] R. J. Hasan and H. N. Abdullah, "Comparative study of selected subcarrier index modulation OFDM schemes," *TELKOMNIKA (Telecommunication Comput. Electron. Control)*, vol. 17, no. 1, pp. 15–22, Feb. 2019, doi: 10.12928/TELKOMNIKA.v17i1.10317.

[24] Q. Li, M. Wen, Y. Zhang, J. Li, F. Chen, and F. Ji, "Pilot insertion with index modulation for OFDM-based vehicular communications," in *2018 IEEE Global Conference on Signal and Information Processing, GlobalSIP 2018 - Proceedings*, 2019, pp. 1204–1208, doi: 10.1109/GlobalSIP.2018.8646384.

[25] A. Alqatawneh and L. Tarawneh, "OFDM system with half-symbol-spaced receiver and channel acquisition error over multipath fading channels," *Jordan J. Electr. Eng.*, vol. 7, no. 2, p. 96, 2021, doi: 10.5455/jjee.204-1613432117.

[26] C. Xiao, J. Wu, S. Y. Leong, Y. R. Zheng, and K. Ben Letaief, "A discrete-time model for triply selective MIMO rayleigh fading channels," *IEEE Trans. Wirel. Commun.*, vol. 3, no. 5, pp. 1678–1688, 2004, doi: 10.1109/TWC.2004.833444.

[27] J. Wu and Y. R. Zheng, "Oversampled orthogonal frequency division multiplexing in doubly selective fading channels," *IEEE Trans. Commun.*, vol. 59, no. 3, pp. 815–822, 2011, doi: 10.1109/TCOMM.2011.121410.090655.

[28] W. Zhou, J. Wu, and P. Fan, "On the maximum Doppler diversity of high mobility systems with imperfect channel state information," in *IEEE International Conference on Communications*, vol. 2015-Septe, 2015, pp. 4431–4436, doi: 10.1109/ICC.2015.7249020.

[29] M. A. Mahamadu, J. Wu, Z. Ma, W. Zhou, Y. Tang, and P. Fan, "Fundamental tradeoff between doppler diversity and channel estimation errors in SIMO high mobility communication systems," *IEEE Access*, vol. 6, pp. 21867–21878, 2018, doi: 10.1109/ACCESS.2018.2826438.

[30] J. Wu, C. Xiao, and N. C. Beaulieu, "Optimal diversity combining based on noisy channel estimation," in *IEEE International Conference on Communications*, vol. 1, 2004, pp. 214–218, doi: 10.1109/icc.2004.1312482.

[31] S. M. Blinder, *Guide to essential math: A review for physics, chemistry and engineering students*, 2nd ed. Elsevier, 2013.

BIOGRAPHY OF AUTHOR

Ali Alqatawneh 🆔 📊 SC Ⓟ is an Assistant Professor at Department of Communication, Electronics and Computer Engineering at Technical Technical University, Jordan. He received the B.Sc. degree in communication engineering from the Mutah University, Jordan, the M.Sc. degree in communication engineering from Mutah University, and the PhD degree in Electrical Engineering with specialization in wireless communication from the university of Arkansas, USA. His research experience covers various topics in wireless communications such as: multicarrier multiple access techniques, channel estimation techniques, high mobility wireless communications, cognitive radio networks, and orthogonal frequency division multiplexing with index modulation. He can be contacted at email: ali.qatawneh@ttu.edu.jo.